Materiales de Construcción
76 (361), January-March 2026, e404
ISSN-L: 0465-2746, eISSN: 1988-3226
https://doi.org/10.3989/mc.2026.396224

ARTICLE

Mechanical performance of a warm-mix asphalt using sodium silicate-modified asphalt and recycled concrete aggregate

Desempeño mecánico de una mezcla asfáltica tibia usando asfalto modificado con silicato de sodio y áridos de hormigón reciclado

H.A. Rondón-Quintana
Facultad del Medio Ambiente y Recursos Naturales, Universidad Distrital Francisco José de Caldas, (Bogotá, Colombia)
Corresponding author: harondonq@udistrital.edu.co, https://orcid.org/0000-0003-2946-9411

W.D. Fernández-Gómez
Facultad del Medio Ambiente y Recursos Naturales, Universidad Distrital Francisco José de Caldas, (Bogotá, Colombia)
https://orcid.org/0000-0001-6339-8050

E.H. Sánchez-Cotte
Facultad Tecnológica, Universidad Distrital Francisco José de Caldas, (Bogotá, Colombia)
https://orcid.org/0000-0001-7370-8745

Abstract: The present study evaluated the mechanical performance of a warm-mix asphalt (WMA) by partially replacing the coarse fraction of natural aggregates (NA) with recycled concrete aggregates – RCA. To manufacture the WMA, a sodium silicate (SS) was used to modify and foam the asphalt cement (AC). SS is presented as a novel additive that has not been investigated by the technical and academic community. Based on penetration and softening point tests carried out on modified AC in different proportions (SS/AC=0.25, 0.50, 0.75, 1.0, 1.25, 1.50% by mass), a content of SS/AC=1% was defined as optimum. Viscosity tests, rheological characterization, and Scanning Electron Microscope (SEM) observations were performed on the modified and unmodified AC. Marshall, Indirect Tensile Strength – ITS, resilient modulus, permanent deformation, fatigue, and Cantabro tests were carried out on the asphalt mixtures. The SS allows a 20°C reduction in the mixing temperature, generating WMA mixes that exhibit similar or even better performance compared to the Control HMA. The mixes with RCA exhibited higher resistance in the Marshall test and similar resistance to permanent deformation with respect to the Control mix, but lower resistance to indirect tension, raveling, fatigue and moisture damage.

Keywords: Warm-Mix asphalt; WMA; Sodium silicate; Hot-mix asphalt; HMA; Recycled concrete aggregate; RCA.

Resumen: El presente estudio evaluó el desempeño mecánico de una mezcla asfáltica tibia (MAT) remplazando parcialmente la fracción gruesa del árido natural (AN) por árido de hormigón reciclado – ACR. Para fabricar la MAT, se utilizó un silicato de sodio (SS), el cual espumó y modificó el cemento asfáltico (CA). El SS se presenta como un aditivo novedoso que no ha sido investigado por la comunidad técnica y académica. Con base en ensayos de penetración y punto de ablandamiento realizados sobre el CA modificado en diversas proporciones (SS/CA=0.25, 0.50, 0.75, 1.0, 1.25, 1.50% en masa) se definió un contenido de SS/CA=1% como óptimo. Sobre el CA modificado y sin modificar se realizaron ensayos de viscosidad, caracterización reológica y observaciones en un microscopio electrónico de barrido (MEB). Sobre las mezclas asfálticas se llevaron a cabo ensayos Marshall, Resistencia en Tensión Indirecta – RTI, Cantabro, módulo resiliente, deformación permanente y fatiga. El SS permite disminuir la temperatura de mezcla en 20°C, generando MATs que experimentan similar e incluso mejor desempeño en ciertas propiedades comparada con la MDC de Control. Las mezclas con ACR exhiben mayor resistencia en el ensayo Marshall y similar resistencia a la deformación permanente con respecto a la mezcla de control, pero menor resistencia en tensión indirecta, al desgaste Cantabro, a la fatiga y al daño por humedad.

Palabras clave: Mezcla asfáltica tibia; MAT; Silicato de sodio; Mezcla densa en caliente; MDC; Árido de hormigón reciclado; ACR.

Received: 09-10-2024 / **Accepted**: 13-07-2025 / **Published**: 29-06-2026

Citation: Rondón-Quintana HA, Fernández-Gómez WD, Sánchez-Cotte EH. 2026. Mechanical performance of a Warm-Mix Asphalt using sodium silicate-modified asphalt and recycled concrete aggregate. *Mater. Construcc.* 76(361): e404. https://doi.org/10.3989/mc.2026.396224

Supplementary information ↓

1. INTRODUCTION

The current trend in road projects is to use environmentally friendly materials. During the construction of asphalt layers, hot-mix asphalts (HMA) are generally used. This material has a negative impact on the environment since it uses high temperatures during its manufacture and compaction, requiring high energy consumption and the use of fuels that generate greenhouse gas emissions and air pollutants (1–6). At the same time, HMAs use naturally occurring aggregates (NA) whose exploitation also affects the environment (e.g., water and air pollution, deforestation, erosion, loss of fertile soil, modification of relief, visual impact). To reduce these environmental impacts, the use of additives and industrial techniques to reduce manufacturing and compaction temperatures (e.g., warm-mix asphalts – WMA) is promoted, as well as the use of alternative materials from recycling (e.g., construction and demolition wastes – CDW, recycled concrete aggregates - RCA, blast furnace slags, reclaimed asphalt pavement – RAP, steel slags) as a replacement for NA (7–12). The above, always trying to match or improve the mechanical performance of the resulting asphalt mix with respect to traditional HMA mixtures (4, 13–16).

A widely used technique to produce WMA consists of foaming the binder (foaming-based WMA techniques) to facilitate the covering of aggregates, optimizing the workability and compaction of the asphalt mix while decreasing the manufacturing temperature and promoting sustainable development (3, 17, 18). Organic or chemical additives and various industrial techniques can be used for this purpose (15). Zeolite-type additives widely known and used are Advera® (sodium aluminum silicate hydrate) and aspha-min® (natrium-aluminum silicate) (17, 19). Both hydrothermally crystallized additives contain a small amount of water (between 18 to 22% by mass), which is released at temperatures above 85°C when mixed with the binder for foaming (20, 21). An additive like those mentioned is sodium silicate (SS) or liquid Na_2SiO_3 (commonly called water glass). This is produced when Na_2CO_3 (sodium carbonate) is chemically reacted with SiO_2 (silicon oxide) and water is added. It is an alkaline material (PH>10), whose approximate density varies between 1300 and 1.600 kg/m^3 (20°C), containing concentrations of Na_2SiO_3 between 35%-45% and water between 55%-65%. The molar concentration of SiO_2/Na_2O ranges from 1.5 to 4.0. Increasing this ratio lowers the pH and raises the viscosity. The literature describes it as an inorganic material or substance that is hydrophobic, a corrosion inhibitor and alkalinity controller (22), environmentally friendly, non-toxic and non-harmful, non-flammable, non-explosive, and cost-effective (23–27). It has high bonding strength, good acid resistance, and heat resistance (28), is impermeable upon hardening, has good bonding ability (29), and good adhesive properties (30). It has been extensively studied in concretes to decrease air-entrained voids, as a setting accelerant and waterproofing agent (28, 31, 32). It has also been used in geopolymerization technology (33) and to stabilize soils (34–37). On the other hand, SiO_2 present in SS is a versatile and valuable component that provides chemical stability, is used as a binder in various applications, highly heat resistant, relatively safe for the environment, non-toxic, and could be useful for improving the rheological properties of asphalt binders at high temperatures, increasing stiffness under monotonic and cyclic loading and resistance to moisture damage of asphalt mixtures (38–40). Regarding Na_2O, its effects on the properties of binders and asphalt mixes have not been identified in the reference literature. However, Na_2O provides alkalinity (41) and improves the shear strength of glass (42).

On the other hand, RCA is a widely studied material as a replacement for NA in various road projects and comes from CDW (43, 44). This residue is found in high quantities, as concrete is one of the most widely used materials in construction projects (45, 46). According to Al-Bayati *et al.* (47), it is generally composed of NA (between 65% to 70%) and coating mortar (between 30% to 35%). According to Le and Bui (48), the lack of control and management of this waste reduces the capacity of landfills and disposal sites, contaminates water sources, changes land use, and does not help promote the reuse and recycling of materials to generate a circular economy (49). In the case of HMA, RCA is reported as a promising material to decrease NA exploitation and consumption (reducing CO_2 emissions; 50). They are also promoted as materials that offer economic, environmental, and social benefits (51, 52). Most studies using RCA instead of NA find that the volumetric and strength parameters of RCA mixes meet quality requirements for roads with low traffic. Regarding performance and durability aspects, the reference literature is contradictory in reporting the influence of RCA. This is mainly due to the heterogeneous nature of this alternative material (11, 53). Some consensuses found in the literature are (50, 52, 54, 55): (i) RCA promotes increased binder content in mixtures due to higher surface porosity; (ii) an optimal percentage of RCA in asphalt mixtures has not been established; iii) It is generally recommended to replace the coarse fraction of NA with RCA (the fine fraction of RCA generally has a lower specific gravity, higher absorption and lower strength than the coarse fraction, thus increasing the asphalt binder content); iv) RCA show lower mechanical strength than NA, but have beneficial physicochemical properties in terms of adhesion and compatibility with the binder (e. g., high CaO content, high porosity and surface texture), as well as optimal geometry (e.g., angular particles and low content of elongated and flattened particles).

The main objective of the present study was to evaluate the performance of a WMA produced with a binder modified with a novel low-cost commercial additive such as SS, which has not been investigated (no studies on the use of SS as an asphalt binder modifier are reported in the literature), and in that sense, it is a contribution to the state of knowledge on the subject. Another objective of the study was to evaluate the performance of WMA by partially replacing the coarse fraction of NA with RCA. This was done to obtain a more environmentally friendly sustainable asphalt mix. In the case of RCA, its usage as a partial replacement for NA in WMA has been gaining attention in the literature and is considered a viable alternative to increase sustainability (8). The understanding and design of asphalt mixes containing RCA to meet desired performance properties still pose various challenges and uncertainties for the technical and academic community (52), and these uncertainties are greater for the case of WMA mixtures incorporating RCA, as they have been less studied (the literature reports few case studies; (9, 10)), and have not yet been widely used in the industry (8). To meet the proposed objectives, an experimental phase was initially designed and carried out to find the optimum SS content of the modified asphalt binder. Viscosity tests, rheological performance, and visualizations in a scanning electron microscope (SEM) were performed on the modified binder. The decrease in temperature to manufacture WMA was obtained by performing Marshall, ITS, and Cantabro tests on asphalt mixtures manufactured with the modified binder. HMA and WMA were then manufactured by partially replacing the coarse fraction of the NA with RCA, and properties under monotonic loading (Marshall and ITS tests), cyclic loading (resilient modulus - RM, resistance to permanent deformation and fatigue under stress-controlled), resistance to moisture damage (calculating the Tensile Strength Ratio – *TSR* parameter) and abrasive resistance (Cantabro test) were evaluated on these mixtures. To evaluate whether SS and RCA generated statistically significant changes in the properties evaluated, an ANOVA analysis of variance (F-test) with 95% confidence was performed (for the analysis, $F_T > F_{0.05}$ means that the change in the measured parameter was statistically significant).

2. MATERIALS AND METHODS

2.1. Materials

The asphalt binder type AC 60/70 (penetration range in dmm; ASTM D5) was supplied by MPI (Manufacturas y Procesos Industriales) and its properties are shown in Table 1.

Table 1. Asphalt binder properties.

Test	Unit	Method	Result	Recommended
Penetration	0.1 mm	ASTM D5	61.3	60 – 70
Softening point	°C	ASTM D36	48.8	48 – 54
Penetration Index	-	NLT 181	-1.034	-1.2 to +0.6
Specific gravity	-	AASHTO T 228	1.024	-
Viscosity (135°C)	P	ASTM D 4402	7.50	4 minimum
Ductility (25°C, 5cm/min)	cm	ASTM D113	135	100 minimum
Flash and fire points	°C	ASTM (2001a)	290	230 minimum
After rolling thin film oven test – RTFOT				
Mass loss	%	ASTM D2872	0.25	0.8 maximum
Penetration (after RTFOT/neat)	%	ASTM D5	80.2	50 minimum
Increase in softening point	°C	ASTM D36	2.6	9 maximum

The NA and RCA (Figure 1) come from companies authorized by the Instituto de Desarrollo Urbano (IDU) in Bogotá (see properties of both materials in Table 2). RCA has lower resistance to abrasive wear and fracture than NA. This is mainly due to the higher porosity of the RCA surface and to the detachment of the adhered mortar, which is fragile and brittle (53, 54). Regarding disintegration in the soundness test, the RCA presented a value higher than the NA, which is attributed to the high detachment of the coating mortar during the test. The values of the elongation and flattening indices can be considered relatively low, inferring that there is a predominance of cubic-shaped particles. This may be a result of the crushing and size reduction process of the RCA during its recycling process, which is evidenced in the fractured particle test results. The RCA reports a higher value of absorption percentage than the NA. This will generate a higher consumption of asphalt binder in the mix (56), and in conjunction with the presence of mortar will promote low specific gravity values (54).

a) b)

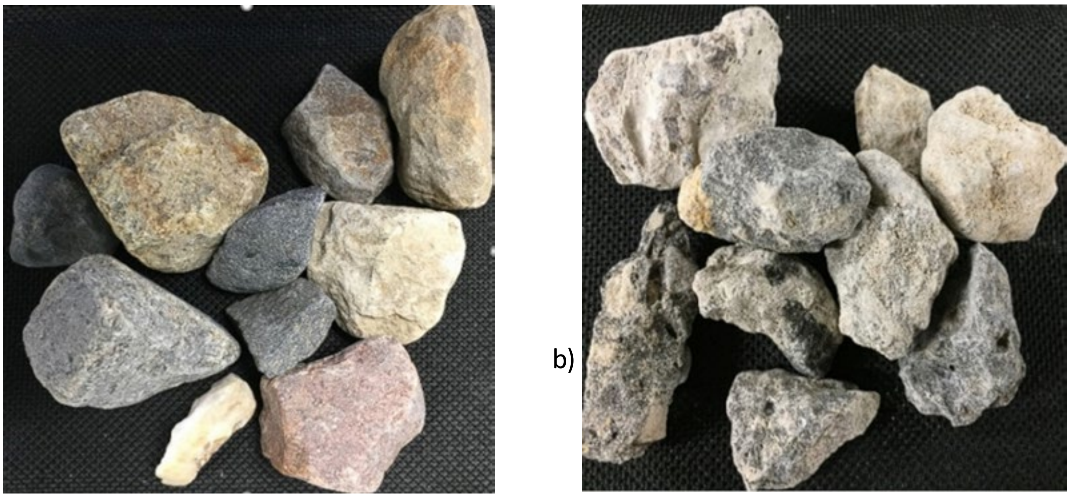

Figure 1. a) NA and b) RCA particles.

Table 2. Aggregate properties.

Test	Method	Recommended	NA	RCA
Specific gravity (coarse aggregate)	AASHTO T 85	-	2.623	2.477
Absorption (coarse aggregate)	AASHTO T 85	-	1.78%	3.92%
Specific gravity (fine aggregate)	AASHTO T 84	-	2.580	-
Absorption (fine aggregate)	AASHTO T 84	-	1.72%	-
Soundness (magnesium sulphate)	AASHTO T 104	18.0% maximum	3.7%	22.2%
Fractured particles (1 side)	ASTM D5821	85% minimum	95.1%	100%
Flat and elongated particles	ASTM D 4791	10% maximum	8.7%	2.1%
Abrasion in Los Angeles machine	AASHTO T 96	25% maximum	21.1%	31.7%
Micro-Deval	AASHTO T 327	20% maximum	17.6%	25.2%
10% of fines (dry resistance)	DNER-ME 096	110 kN minimum	129.0 kN	107.3 kN
10% of fines (wet resistance)	DNER-ME 096	82.5 kN minimum	115.2 kN	91.3 kN
10% of fines (wet/dry ratio)	DNER-ME 096	75% minimum	89.3%	85.1%

The surfaces of the NA and mortar adhered to the RCA were observed in a SEM (JEOL JSM-6700F) with a working distance of approximately 4 to 9 mm, accelerating voltage between 4 to 20 kV, and magnifications between 500 and 40,000 (Figures 2a and b, respectively). The elemental chemical composition was also determined on these surfaces (Table 3). The surface of the mortar bonded to the RCA shows higher porosity and roughness than that of the NA. In addition, the adhered mortar has a chemical composition like cement and a higher Ca/Si content than the NA. All the above could help increase compatibility with the asphalt binder and improve adhesion (57, 58). Despite the above, SEM visualizations show that the adhered mortar can detach due to the presence of cracks and micro-cracks in the RCA (11, 53, 55; Figure 3).

a) b)

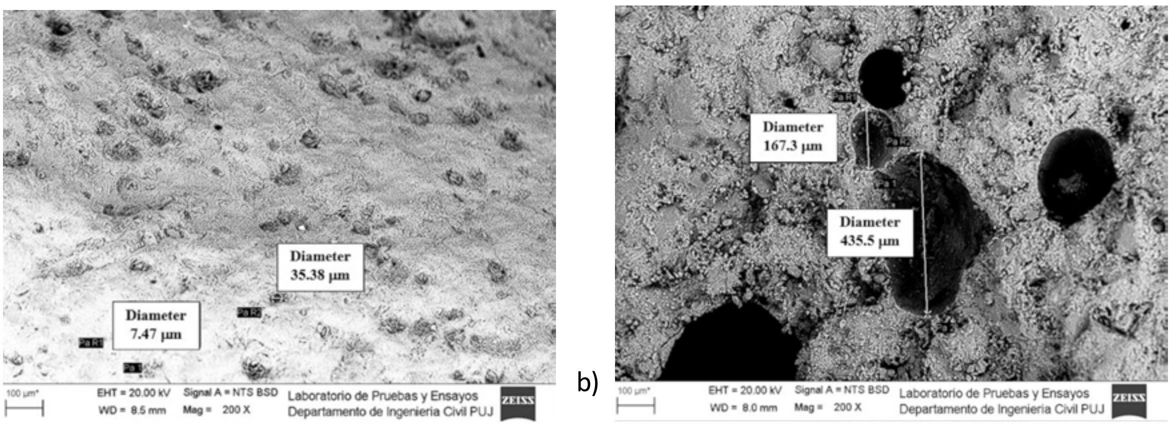

Figure 2. SEM observations: a) NA and b) RCA surface.

Table 3. Elemental composition of particles based on SEM.

Particle	C	O	Ca	Mn	Si	Al	Fe	Mg	K	Ti
Adhered mortar	16.14	51.87	15.32	0.16	12.12	3.10	0.87	0.28	0.15	-
NA	-	48.30	0.33	-	41.26	2.82	6.32	0.38	0.32	0.27

The SS was supplied by Químicos Campota y CIA. LTDA in Bogotá and is sold over the counter (cost approximately US$ 2.9/liter). It is an alkaline liquid chemical (PH=12) of a transparent grayish color. At 20°C its density and viscosity are 1.49 g/ml and 758 cP, respectively. The ratio SiO_2/Na_2O = 2.4 (SiO_2=31.8% and Na_2O=13.2%, approximately).

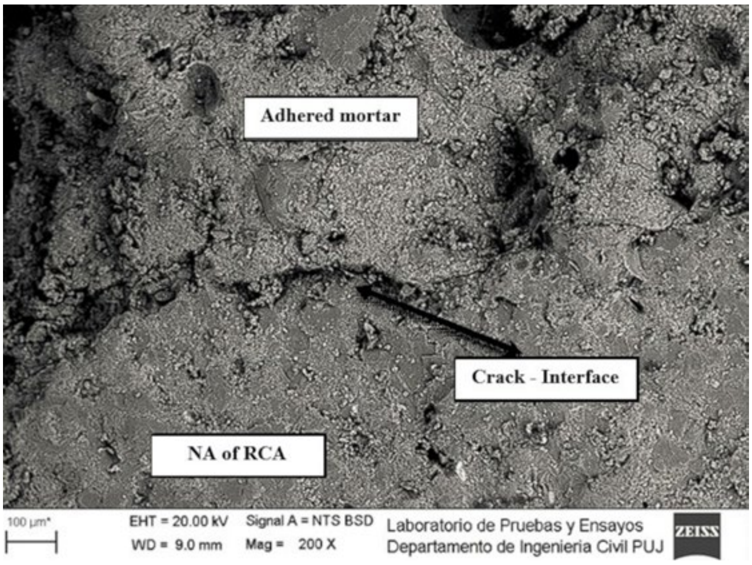

Figure 3. Fissures and microcracks in the adhered mortar.

2.2. Modified asphalt binder

To initiate the modification process of AC 60/70, SS was placed on its surface at laboratory room temperature (Figure 4a). The SS/AC ratios were 0.25, 0.50, 0.75, 1.0, 1.25, and 1.50% with respect to mass. These ratios were chosen by trial and error and considering recommended percentages with other water-bearing additives (e.g., Aspha-min® and Advera®; (16, 17, 59). As a second step, both the binder and SS were heated using a laboratory stove and both materials were mixed when AC 60/70 reached its softening point. At approximately 80°C, the SS foamed the binder (Figure 4b), and under this temperature, the mixing process was continued with a laboratory spatula for a short time (30 seconds) to avoid losing the foaming process. In addition, under real production conditions in an asphalt plant, the SS must be added at the same instant that the aggregates are mixed with the binder.

a)  b) 

Figure 4. a) SS on its binder surface; b) foaming of the binder at 80°C.

Softening point (ASTM D36) and penetration (ASTM D5) tests were performed on modified (SS/AC=0.25, 0.50, 0.75, 1.0, 1.25, and 1.50%) and unmodified (SS/AC=0%) AC 60/70 (Figure 5). A higher binder stiffness is observed when modified with 1% SS (softening point increases and penetration decreases). This SS/AC=1% ratio was chosen to fabricate the WMA in future experimental phases.

Viscosity tests using a rotational viscometer (ASTM D 4402; Figure 6) and rheological characterization at intermediate and high service temperatures using a dynamic shear rheometer – DSR (AASHTO T 315; Table 4) were performed on modified (SS/AC=1%) and unmodified (SS/AC=0%) asphalt. The shear complex modulus (G^*) and phase angle (δ) were measured in the DSR. To evaluate the performance grade (PG) and resistance to rutting at high temperature, the $G^*/\sin\delta$ ratio was used (the criterion used was $G^*/\sin\delta > 1.0$ kPa for virgin asphalt and $G^*/\sin\delta \geq 2.2$ kPa for after RTFOT). For the case of cracking resistance at intermediate temperatures, the parameter $G^*\sin\delta$ was used (the criterion used was $G^*\sin\delta \leq 5000$ kPa after RTFOT+PAV). Viscosity tends to decrease slightly when SS is used as an additive (Figure 6) mainly because during the test the foaming effect is lost when the temperature exceeds 100°C (water boils and is expelled from the SS; (59, 60)). Both binders (modified and unmodified) exhibit equal PG at high and intermediate temperatures (64°C and 22°C, respectively), i.e., SS did not generate significant changes in the rheological properties of the binder. However, Table 4 shows that SS tends to increase the binder stiffness, which is consistent with the penetration and softening point results (Figure 5). Also, SS tends to decrease binder stiffness when exposed to short-term (RTFOT) and long-term (RTFOT+PAV) aging processes, which is an indicator of possible increase in aging resistance.

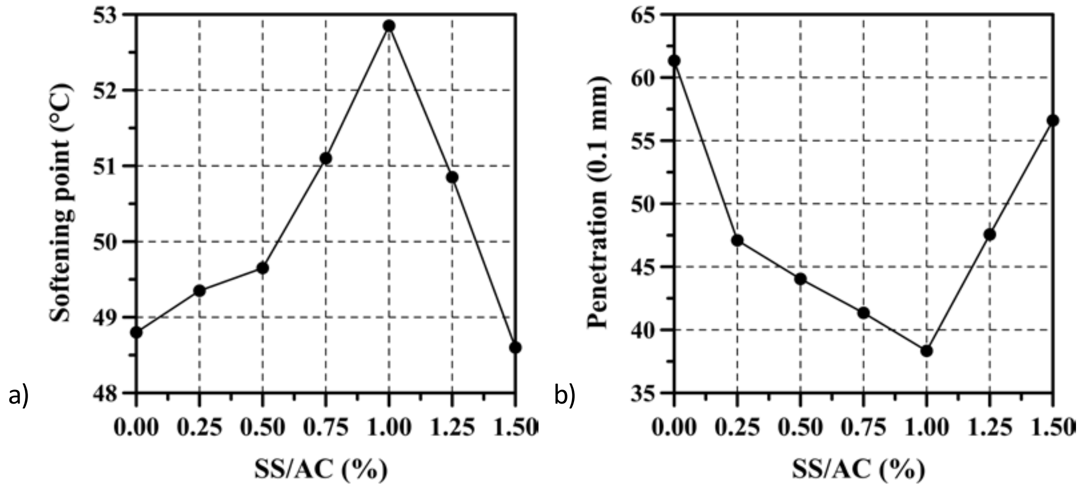

Figure 5. a) softening point and b) penetration with SS/AC ratio.

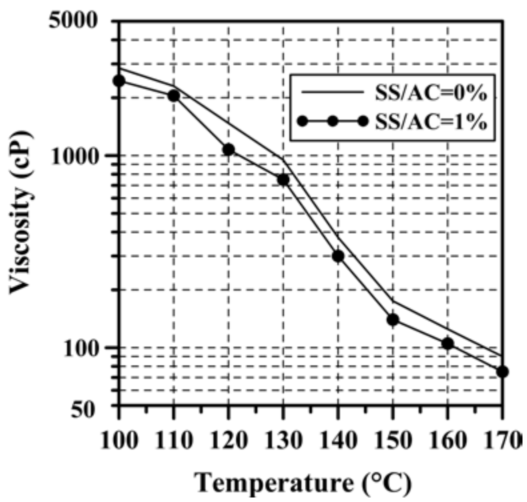

Figure 6. Viscosity curve of AC 60/70 unmodified (SS/AC=0%) and modified (SS/AC=1%).

SEM observations were made on both binders (modified and unmodified) and the elemental chemical composition was measured (Table 5). Images of both binders are not presented, since only dark black background is observed, without any change, indicating that SS is adequately distributed and homogenized in AC 60/70. The chemical composition of the modified binder (SS/AC=1%) is in accordance with the modification percentage and the SiO_2/Na_2O ratio of SS, showing that the additive was homogeneously mixed in the binder. On the other hand, the elemental chemical composition did not change, i.e., no chemical reaction is reported.

Table 4. Summary of rheology test results.

Temperature (°C)	Frequency (rad/s)	|G*|/sinδ (kPa) SS/AC=0%	|G*| · sinδ (kPa) SS/AC=0%	|G*|/sinδ (kPa) SS/AC=1%	|G*| · sinδ (kPa) SS/AC=1%
Virgin asphalt binder					
58	10	3.12 ± 0.61	3.09	3.31 ± 0.65	3.27
64	10	1.32 ± 0.26	1.31	1.52 ± 0.30	1.51
70	10	0.609 ± 0.12	0.607	0.695 ± 0.14	0.69
After RTFOT					
58	10	9.59 ± 1.88	9.14	9.48 ± 1.85	9.06
64	10	4.11 ± 0.81	3.99	4.05 ± 0.79	3.94
70	10	1.81 ± 0.36	1.78	1.82 ± 0.36	1.79
After RTFOT + PAV (Pressure Aging Vessel)					
19	10	18112 ± 3549	6174.4	17193 ± 3369	5755.1
22	10	13350 ± 2616	4911.6	12803 ± 2509	4552.8
25	10	9221 ± 1807	3605.9	9007 ± 1765	3458.5

Table 5. Elemental chemical composition of the additive and binders (modified and unmodified).

Material	Chemical element (%)				
	C	O	S	Si	Na
SS	-	56.6±1.53	-	27.7±1.28	15.7±0.49
SS/AC=0%	99.0±0.13	-	1.0±0.13	-	-
SS/AC=1%	97.9±0.1	-	1.1±0.10	0.8±0.14	0.3±0.12

2.3. Control mix design and RCA mixes

As Control HMA (SS/AC=0%), the HMA recommended by INVIAS (61) was used to construct wearing course asphalt layers (the gradation is shown in Figure 7). This mix was designed using the Marshall method (AASHTO T-245). The optimum asphalt binder content (OAC) was 5.5% (Table 6) and was obtained considering the criteria established by INVIAS (61). The samples were compacted at 75 blows per face and three samples were used for each asphalt content. 150°C and 145°C were used as mixing (MT) and compaction (CT) temperatures, respectively (obtained from the viscosity curve, Figure 6). The Marshall strength parameters (stability – *S*, Flow – *F*, and *S/F* ratio) were obtained on samples conditioned at 60°C, applying a loading rate of 50 mm/minute in the Marshall equipment. The volumetric parameters (voids in the total mix – *VTM*, void in the mineral aggregate – *VMA*, voids filled with asphalt – *VFA*) were obtained following the guidelines established by AASHTO T-245.

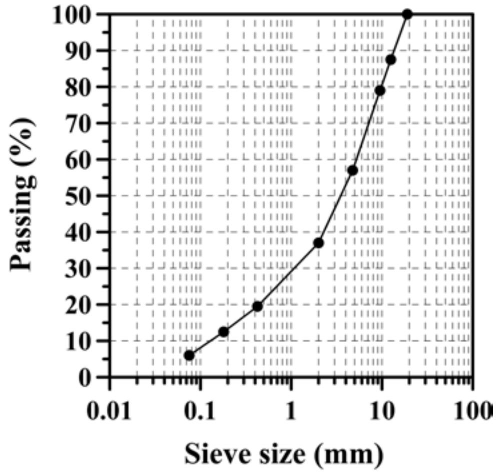

Figure 7. Gradation of Control HMA.

Table 6. Marshall test results (HMA Control).

AC content (%)	*VTM* (%)	*VFA* (%)	*VMA* (%)	*S* (kN)	*F* (mm)	*S/F* (kN/mm)
4.5	6.32	61.33	16.33	13.86	3.73	3.72
5.0	5.28	67.91	16.44	15.51	3.64	4.26
5.5	3.91	75.99	16.27	15.78	3.47	4.55
6.0	1.82	88.29	15.50	15.95	3.85	4.14

2.4. Choice of the MT to manufacture the WMA

New Marshall samples using OAC=5.5% were manufactured to evaluate the influence of MT (150, 140, 130, 120 and 110°C) on unmodified (Control, SS/AC=0%) and modified (SS/AC=1.0%) HMA. The above to perform Marshall (AASHTO T-245), ITS (AASHTO T 283) and Cantabro (Tex-245-F) tests. Three samples per type of mix and per MT were manufactured for the Marshall and Cantabro tests. In the case of the ITS test, six samples per type of mix and per each MT were manufactured (three to evaluate the resistance under dry condition – *ITSD*, and three conditioned or partially saturated – *ITSC*). The Marshall test was performed following the guidelines defined in the previous experimental phase (AASHTO T-245). For the ITS test, the *VTM* of each sample ranged between 7±1%. By calculating the *ITSC/ITSD* ratio (in percent), the *TSR* was obtained. For the ITS, the load was applied at a speed of 50.8 mm/min in the Marshall machine on samples conditioned at 25°C. The Cantabro test was performed on the Los Angeles machine on dry samples conditioned at 20°C, applying 300 revolutions to each sample and following the guidelines established by Tex-245-F. The mass loss or *CL* parameter (Cantabro Loss, in percentage) was calculated by relating the mass loss after applying the 300 revolutions to the initial mass of the sample.

The results of the Marshall, ITS, and Cantabro tests are shown in Figures 8, 9, and 10, respectively. In the Marshall test, an increase in *VTM* is logically observed as MT decreases (Figure 8a), mainly due to the loss of workability and compatibility of the mixes. This increase in porosity (*VTM*) generated a loss of cohesion and a decrease in strength under monotonic loading (*S/F*, Figure 8b). However, the SS helped to decrease the *VTM* (improved the workability and compatibility of the mixes), since the foaming process facilitated the covering of the aggregates. This, together with the increased stiffness of the modified asphalt binder (Figure 5), helped to increase the *S/F* ratio of the modified asphalt mix (on average this increase varied between 12 and 44%). A similar trend is observed in the ITS and Cantabro test results. The decrease in MT generates a decrease in the *ITSD* (Figure 9a) and *ITSC* (Figure 9b) parameters, decreases the resistance to moisture damage (decreases *TSR*, Figure 9c), and abrasion resistance (increases *CL*, Figure 10). By increasing the viscosity of the binder due to the decrease in MT, it becomes challenging to cover the aggregates, leading to a loss of binder-aggregate adhesion. Also in both tests, SS helped to increase the strength parameters *ITSD*, *ITSC* and *TSR* (on average, *ITSD* and *ITSC* increased 11.5±3.3% and 20.5±5.3%, respectively with respect to the Control mix) and decrease the *CL* (average decrease of 13.9±3.8%). The presence of SiO_2 in SS could have helped to increase *ITSD* and *ITSC* (e.g., 62–65). On the other hand, the hydrophobic nature of SS could contribute to increased resistance to moisture damage (29, 31, 40). In addition, SS could help improve binder-aggregate bonding due to its high bonding force (28–29), as well as mixture cohesion and abrasion resistance, raveling and weathering (66–68).

In the Marshall test, the *S/F* ratio and the *VTM* of the modified mixture are like the Control one when decreasing MT by approximately 27 and 20°C, respectively. In the case of the ITS test, the magnitudes of the *ITSD*, *ITSC* and *TSR* parameters of the modified mixes are like the Control when decreasing MT by approximately 20°C, 16 and 10°C, respectively. In the Cantabro test, the approximate decrease is 24°C to achieve similar performance in both mixtures. It is important to highlight that all the properties measured in the Marshall, ITS and Cantabro tests changed significantly from the statistical point of view when SS was used as the asphalt binder modifier (ANOVA, $F_T>F_{0.05}=7.71$; Table 7). Based on the results obtained, MT=130°C was chosen to manufacture the WMA with the SS (20°C decrease with respect to the Control HMA). With this MT, similar or even superior performance is achieved in most of the properties evaluated (except for the *ITSC* and *TSR* parameters).

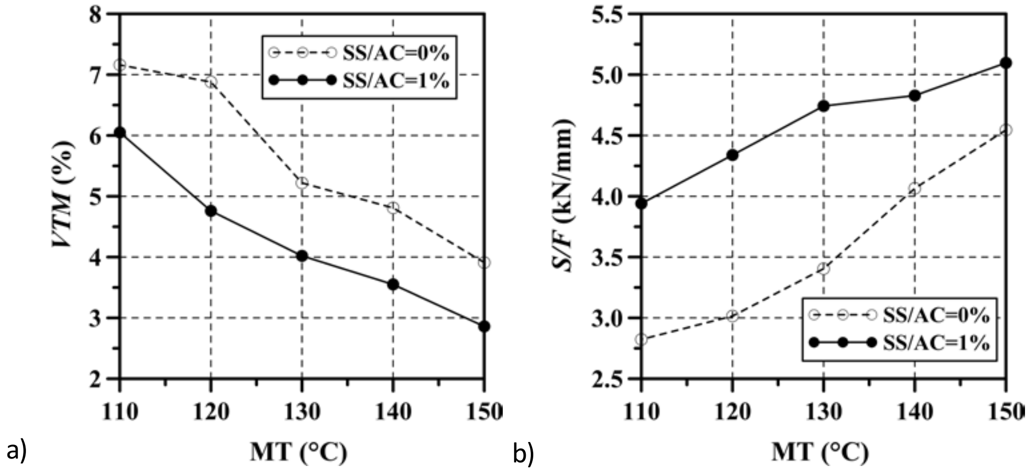

Figure 8. a) VTM and b) S/F ratio evolution with MT.

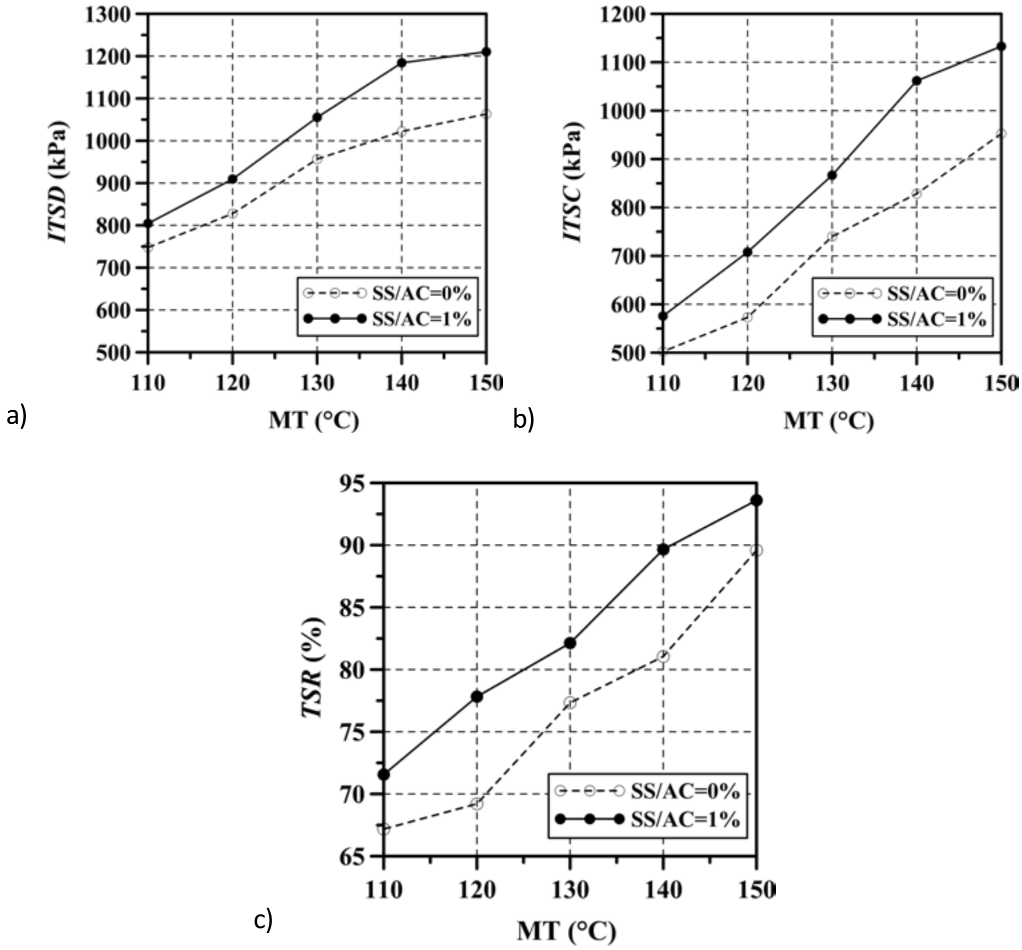

Figure 9. a) ITSD, b) ITSC and c) TSR evolution with MT.

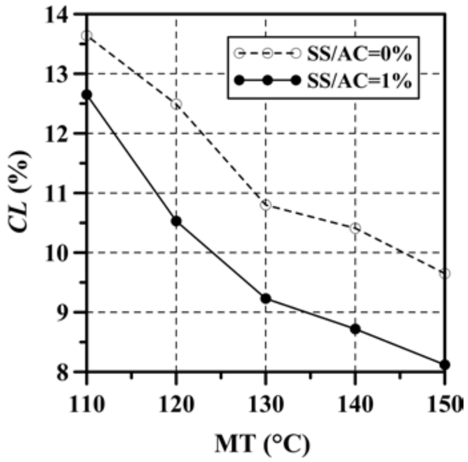

Figure 10. Evolution of *CL* with MT.

Table 7. ANOVA – Marshall, ITS and Cantabro test (SS/AC=0% and 1%).

MT (°C)	*S/F* (kN/mm)	*VTM* (%)	*ITSD* (kPa)	*ITSC* (kPa)	*CL* (%)
			F_T		
150	20.06	27.11	114.6	140.2	73.4
140	56.22	91.14	264.0	344.4	123.7
130	112.72	160.2	83.7	134.3	52.0
120	113.72	160.4	91.7	456.9	98.4
110	27.18	27.97	62.8	68.7	58.3

2.5. Replacement of NA with RCA and mixture design

For the subsequent experimental phase, Marshall-type samples of HMA (MT=150°C; SS/AC=0%) and WMA (MT=130°C; SS/AC=1%) mixes were manufactured by mass replacing 1/2” (12.5% of aggregate) and 1/2”+3/8” (21% of aggregate) NA particles by RCA. Smaller particles were not replaced as recommended in the reference literature (54, 69). Also, these replacement percentages were chosen based on results obtained in previous studies (69–71). To obtain the OAC of the mixes with the replacement of NA by RCA, the Marshall test was performed again following the guidelines established for the design of the Control mix described above. The results are shown in Table 8. The OAC of the mixes with the replacement of 1/2” particles and 1/2”+3/8” particles were 6.0%. The increase in OAC with respect to the Control mix is due to the higher porosity of the RCA-bonded mortar (higher binder absorption). Additionally, the lower specific gravity of the RCA generates an increase in particle volume when mass replacement is performed (higher number of particles to be covered with asphalt binder; (71, 72)). Higher asphalt consumptions in mixes with RCA have been widely identified in the reference literature (54, 71, 73).

Table 8. Marshall test results (replacement of NA with RCA).

AC (%)	*S* (kN)	*F* (mm)	*S/F* (kN/mm)	*VTM* (%)	*VFA* (%)	*VMA* (%)
Replacement 1/2”						
5.0	15.76	3.68	4.28	6.80	61.68	17.71
5.5	17.74	3.57	4.97	4.58	72.72	16.78
6.0	17.31	3.32	5.21	3.59	78.82	16.95
6.5	14.36	4.61	3.11	2.15	87.13	16.74
Replacement 1/2”+3/8”						
5.0	14.47	3.81	3.80	7.01	60.76	17.85
5.5	15.37	3.60	4.27	5.97	66.73	17.94
6.0	15.29	3.18	4.81	4.29	75.48	17.49
6.5	15.32	4.18	3.67	3.61	79.84	17.92

2.6. Mechanical resistance tests

Mechanical resistance tests were performed on six types of mixes: (i) Control HMA (MT=150°C, SS/AC=0%; no replacement of NA by RCA), (ii) WMA (MT=130°C, SS/AC=1%; no replacement of NA by RCA); (iii) HMA-RCA-1/2 (MT=150°C, SS/AC=0%; replacing 1/2" NA particles with RCA); iv) HMA-RCA-1/2+3/8 (MT=150°C, SS/AC=0%; replacing 1/2"+3/8" NA particles with RCA); v) WMA-RCA-1/2 (MT=130°C, SS/AC=1.0%, replacing 1/2" particles of the NA with RCA); vi) WMA-RCA-1/2+3/8 (MT=130°C, SS/AC=1.0%, replacing 1/2"+3/8" particles of the NA with RCA).

To evaluate mechanical performance under monotonic loading, Marshall and ITS tests were performed. Resistance to moisture damage and abrasion resistance were evaluated by calculating the *TSR* and *CL* parameters, respectively. These tests were performed as described in the previous experimental phases. To evaluate the performance under cyclic loading, RM (UNE-EN 12697-26), permanent deformation (UNE-EN 12697-25), and fatigue resistance (UNE-EN 12697-24) tests were performed in a Nottingham Asphalt Tester (NAT). The RMs were obtained at three temperatures (10, 20 and 30°C) and loading frequencies (2.5, 5.0 and 10.0 Hz). To conduct this test, nine specimens were prepared. The resistance to permanent deformation was measured at 40°C, applying 3600 loading cycles (loading frequency of 0.5 Hz and square wave), and stress magnitude of 100 kPa. The accumulation of the displacement with the number of cycles obtained on the samples was averaged from three samples per type of mixture. Fatigue tests were performed under stress-controlled loading mode (loading frequency of 10 Hz and stresses varied between 120 and 600 kPa). The specimens were conditioned at 20°C. The number of load cycles to failure (*N*) was obtained when the specimens reached complete failure during the test.

3. RESULTS AND DISCUSSION

3.1. Marshall, ITS and Cantabro tests

The results of the Marshall, ITS, and Cantabro tests are shown in Figures 11, 12, and 13, respectively. The *S/F* ratio increases slightly (between 1 and 3%) with the inclusion of SS. This is despite the fact that the mixture was produced by lowering the MT by 20°C. However, these increases are not statistically significant according to ANOVA analysis (Table 9). The replacement of the 1/2" particles of NA by RCA increased the *S/F* ratio between 13 and 15% and these increases were statistically significant. In the case of the replacement of 1/2"+3/8" particles, this increase was lower (6% on average) and was not statistically significant (Table 9). On the other hand, the parameters *ITSD*, *ITSC*, and *TSR* tend to increase slightly (between 0.7 and 3.9%) using SS but are not statistically significant (only one case was significant in the analysis, see Table 9). This indicates that SS tends to increase the indirect tensile strength and moisture damage, but from a statistical point of view the values are similar. On the contrary, the replacement of NA particles by RCA contributes to decrease the magnitude of these parameters, especially in the presence of water and when more NA is replaced by RCA (under these conditions, the reported changes in the parameters are statistically significant; see Table 9). The *ITSD* for example decreases between 0.1 and 2.4% when 1/2" particles are replaced, while this decrease is approximately 6% when replacing the 1/2"+3/8" fraction. In the case of *ITSC*, the decrease varied between 5 and 10%, and between 11 and 14.2% with the replacement of 1/2" and 1/2"+3/8" particles, respectively. This generated a notorious decrease in moisture damage resistance (*TSR* decreased between 5 and 8%, and between 6 and 9% when 1/2" and 1/2"+3/8" particles were replaced, respectively). The decrease in these parameters may be due to insufficient binder to sufficiently cover the increase in RCA particle volume due to mass replacement (56, 69, 74). A similar behavior to the ITS test was observed in the Cantabro test. SS tends to increase abrasion and raveling resistance (*CL* decreases between 2.3 and 13.4%), while RCA tends to decrease it, especially when more replacement is performed (replacement of 1/2" particles and 1/2"+3/8" fraction increase *CL* between 7 and 10.3%, and between 26 and 38%, respectively). Despite the above, the changes in the *CL* parameter tend not to be statistically significant (only for the case of the WMA mixture with 1/2"+3/8" fraction replacement was it significant; see Table 9).

In summary, the SS when foaming the binder is an additive that allows for a 20°C reduction in MT, producing mixtures that exhibit similar mechanical resistance under monotonic load, to moisture damage and abrasion with respect to the Control mixture. In other words, SS helps to improve cohesion and binder-aggregate adhesion. This may be due to the high bonding force of SS, its hydrophobic properties, the presence of SiO_2, and its tendency to increase the stiffness of the base binder (Figure 5, Table 4), as mentioned above. On the contrary, the RCA decreases the mechanical performance evaluated in this experimental phase (except for the *S/F* ratio). This is mainly due to the presence of mortar adhered to the RCA, which is brittle and fragile (52, 54, 73). Likewise, the characterization of RCA (Table 2) shows a material of lower hardness and fracture resistance compared to NA. Also, SEM visualization shows an RCA with presence of cracks that could help to detach the mortar. The slight increase in cohesion (increase in the *S/F* ratio) may be due to the good geometry of the RCA particles, the higher Ca/Si ratio of the RCA (Table 3), and the incorporation of more RCA particles (as a product of the lower specific gravity of the RCA) with good porosity and surface texture (Figure 2), which could have contributed to generate a more frictional granular skeleton (70–72).

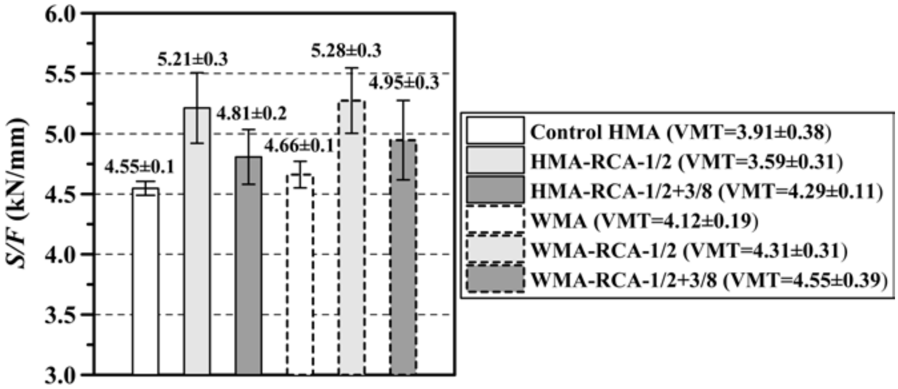

Figure 11. *S/F* ratio - Marshall test results.

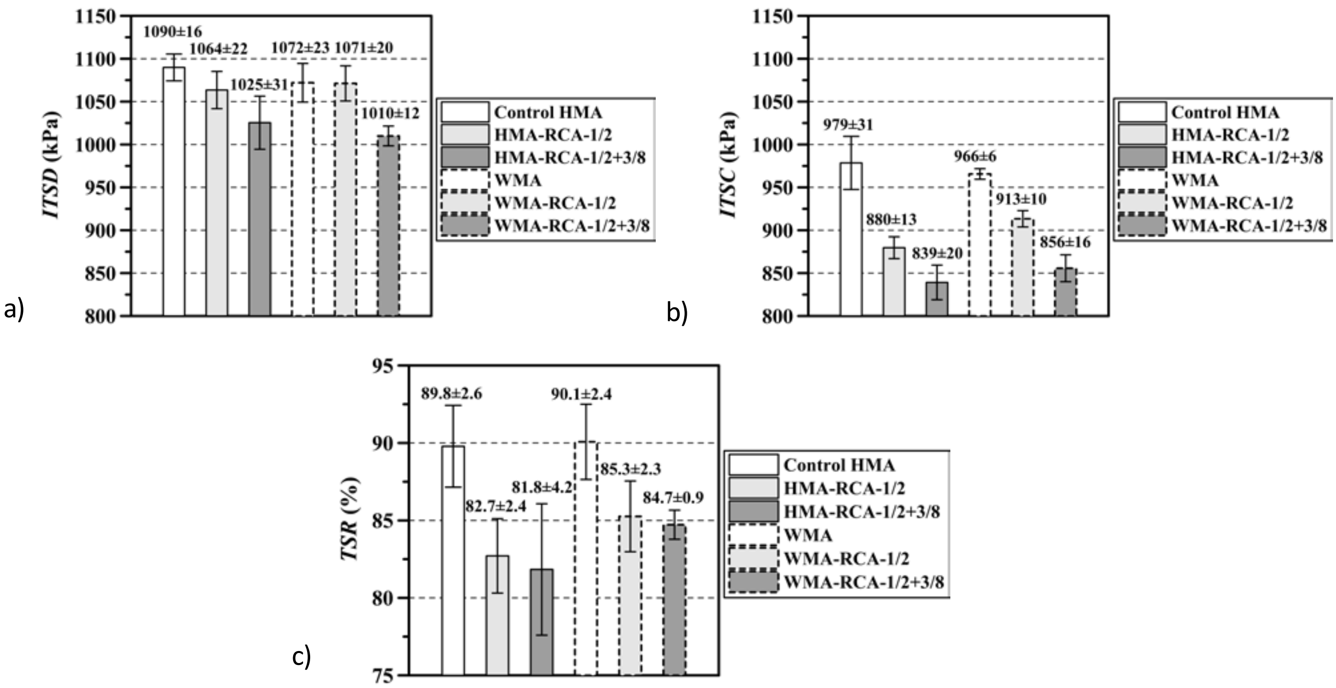

Figure 12. a) *ITSD*, b) *ITSC*, c) *TSR* results.

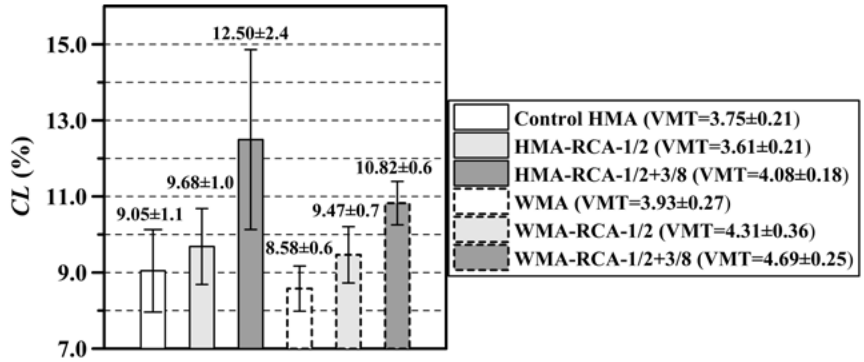

Figure 13. *CL* (%) - Cantabro test results.

Table 9. ANOVA – ITS and Cantabro tests.

Mixtures	*S/F*	*ITSD*	*ITSC*	*TSR*	*CL*
			F_T		
Influence of SS					
HMA vs. WMA	2.76	1.27	0.5	0.02	0.43
HMA-RCA-1/2 vs. WMA-RCA-1/2	0.083	0.20	13.5	1.77	0.09
HMA-RCA-1/2+3/8 vs. WMA-RCA-1/2+3/8	0.390	0.66	1.25	1.25	1.41
Influence of RCA					
HMA vs. HMA-RCA-1/2	15.3	2.92	26.2	11.71	0.56
HMA vs. HMA-RCA-1/2+3/8	3.97	10.4	42.6	7.45	5.28
WMA vs. WMA-RCA-1/2	13.4	0.002	63.7	6.26	2.62
WMA vs. WMA-RCA-1/2+3/8	2.16	18.1	128.0	12.82	22.3

3.2. Resilient modulus and permanent deformation tests

The RM and permanent deformation values are presented in Figures 14 and 15, respectively. When decreasing MT 20°C and using SS, the general tendency of the mixes is to undergo similar stiffness under cyclic loading (for any temperature and loading frequency) and resistance to permanent deformation, with respect to the HMA mixes (the changes in RM and displacement accumulation are not statistically significant when SS is used, see Tables 10 and 11). For the case of RM, the only exception is observed in the mixtures that replaced 1/2”+3/8” of NA by RCA for temperatures of 20 and 30°C. In this condition, SS increases the RM of the mixtures, and this change was statistically significant. These results present SS as a promising additive that allows decreasing MT 20°C, generating mixtures that exhibit similar stiffness (and even higher in some cases) and resistance to permanent deformation under cyclic loading. They are also consistent with the *S/F* ratio and the increase in binder stiffness previously presented due to the presence of SS.

Regarding the influence of RCA as a replacement for NA, contradictory results are presented. The RM tends to decrease markedly when NA is replaced by RCA, and this decrease is greater with increasing replacement. From a statistical point of view, most of these decreases in RM were statistically significant (Table 10). The higher binder content in the mixtures with RCA may have helped to decrease the RM (75–76). Despite the above, the resistance to permanent deformation increased slightly with the presence of RCA in the mixtures (the difference between the highest and the lowest displacement value was only 0.11 mm, and the displacement rates were similar varying between 19x10-6 and 26x10-6 mm/cycle), and this increase was not statistically significant (Table 11). Generally, asphalt mixtures undergo higher resistance to permanent deformation when RM increases. The explanation for this contradiction is not clear. Additionally, the lower hardness and fracture resistance of RCA particles are expected to contribute to increased deformation accumulation. However, the higher *S/F* ratio of the RCA mixtures and the increased number of contacts between particles of the granular skeleton (the lower specific gravity of RCA promoted the incorporation of a greater number of particles) could explain the increase in deformation resistance (54, 77).

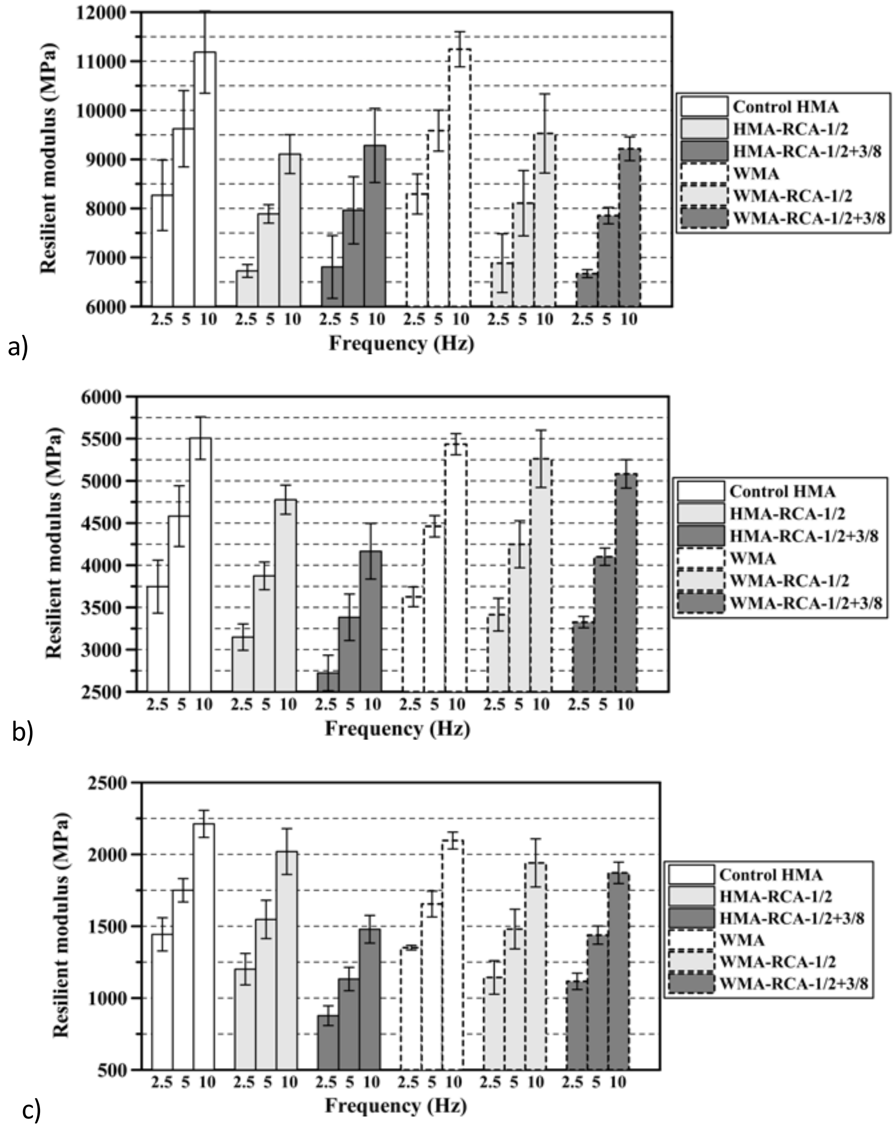

Figure 14. Resilient modulus at a) 10°C, b) 20°C, c) 30°C.

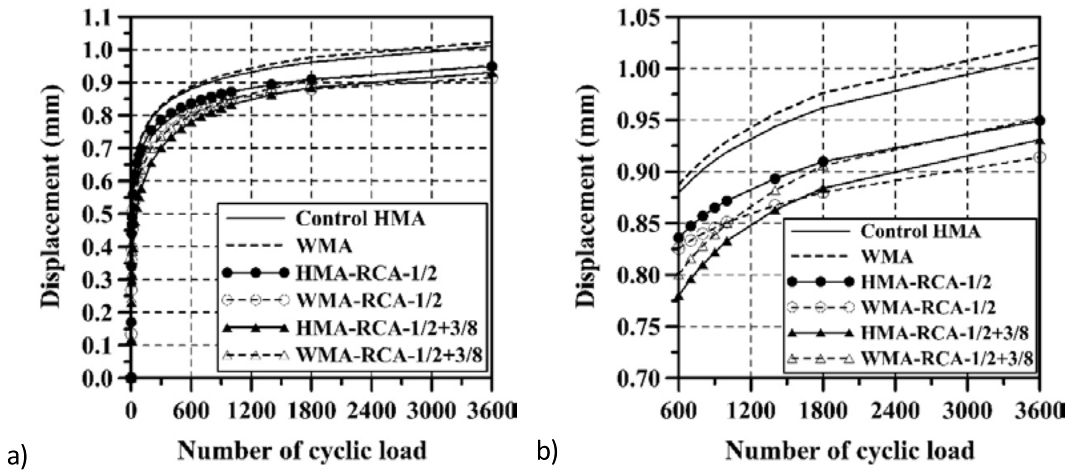

Figure 15. Permanent deformation test: a) full test results, b) results after 3600 cycles.

Table 10. ANOVA – Resilient modulus test.

Mixture	10°C			20°C			30°C		
	2.5Hz	5Hz	10Hz	2.5Hz	5Hz	10Hz	2.5Hz	5Hz	10Hz
Influence of SS									
HMA vs. WMA	0.003	0.006	0.012	0.39	0.30	0.193	1.89	1.86	3.28
HMA-RCA-1/2 vs. WMA-RCA-1/2	0.198	0.30	0.659	3.44	4.04	4.86	0.39	0.36	0.35
HMA-RCA-1/2+3/8 vs. WMA-RCA-1/2+3/8	0.133	0.072	0.021	22.35	17.89	18.41	21.55	26.4	31.19
Influence of RCA									
HMA vs. HMA-RCA-1/2	13.36	14.12	15.09	8.75	9.64	17.08	6.95	5.07	3.24
HMA vs. HMA-RCA-1/2+3/8	6.90	7.72	8.54	22.00	21.02	31.27	53.16	86.67	88.97
WMA vs. WMA-RCA-1/2	11.37	10.61	11.36	2.60	1.46	0.69	9.28	3.34	2.31
WMA vs. WMA-RCA-1/2+3/8	45.43	44.53	66.03	14.66	14.74	8.46	46.92	11.54	16.82

Table 11. ANOVA – Permanent deformation test.

Mixture	Number of cyclic loads	
	1800	3600
	F_T	
Influence of SS		
HMA vs. WMA	0.06	0.04
HMA-RCA-1/2 vs. WMA-RCA-1/2	0.84	0.87
HMA-RCA-1/2+3/8 vs. WMA-RCA-1/2+3/8	0.37	4.59
Influence of RCA		
HMA vs. HMA-RCA-1/2	0.90	1.08
HMA vs. HMA-RCA-1/2+3/8	1.79	2.29
WMA vs. WMA-RCA-1/2	7.06	6.42
WMA vs. WMA-RCA-1/2+3/8	4.10	5.03

3.3. Fatigue test

The curves of the fatigue strength results are presented in Figure 16. These curves are described mathematically using Equation [1]. σ is the stress necessary to determine the number of failure cycles - N, and the parameters k_1 y b (slope of the fatigue law) are obtained by regression. Using Equation [1], the parameters σ_6 y σ_7 (magnitude of stress for the material to fail at N = 10^6 y 10^7, respectively; see Table 12) can be obtained. Higher values of k_1, σ_6 y σ_7, and lower absolute value of b, means increase in fatigue strength in Table 12. SS contributes to a slight increase in fatigue strength. This is even though the WMA is manufactured 20°C lower than the HMA Control mix. On the contrary, the incorporation of RCA in the mixtures tends to decrease the fatigue strength. The trends in the results are consistent with those obtained in ITS and RM tests (under stress-controlled, fatigue strength tends to have a direct correlation with indirect tensile strength and RM; (78–81). Additionally, in the case of RCA, the lower hardness and mechanical strength compared to NA, as well as the presence of micro-cracks in the bonded mortar could affect the fatigue performance of the HMA-RCA and WMA-RCA mixtures. Perhaps an increase in the binder content or pretreatment of the RCA could increase the fatigue strength as has been reported in the reference literature (54). However, this consideration would increase the cost of the mixtures.

$$\sigma = k_1(N)^b \quad [1]$$

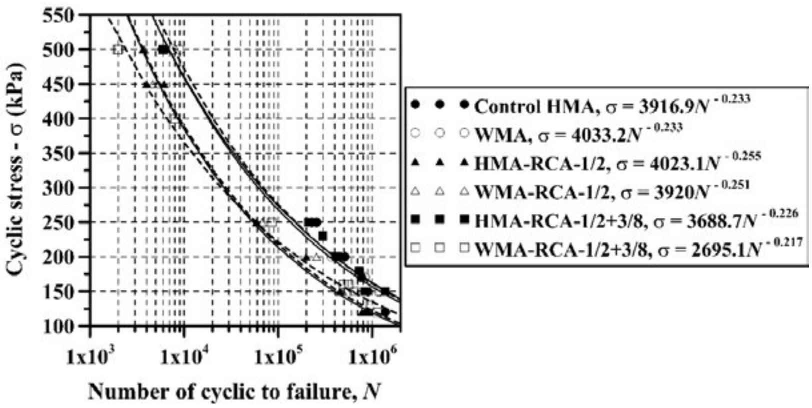

Figure 16. Fatigue test results.

Table 12. *k1*, *b*, σ_6, and σ_7 parameters.

Mixture	*VTM* (%)	R-squared (r^2)	k_1	*b*	σ_6 (kPa)	σ_7 (kPa)
Control HMA	4.3±0.17	0.988	3916.9	-0.233	156.7	91.6
WMA	4.4±0.12	0.993	4033.2	-0.233	161.3	94.3
HMA-RCA-1/2	3.9±0.30	0.991	4023.1	-0.255	118.7	66.0
WMA-RCA-1/2	4.3±0.17	0.994	3920.0	-0.251	122.3	68.6
HMA-RCA-1/2+3/8	4.1±0.19	0.992	3688.7	-0.226	162.5	96.6
WMA-RCA-1/2+3/8	4.3±0.21	0.993	2695.1	-0.217	134.4	81.6

4. CONCLUSIONS

This research evaluated the possible use of a SS as a modifier of an asphalt binder to produce WMA. Likewise, the influence of an RCA on the properties of WMA when used as a partial replacement (1/2” and 1/2”+3/8” particles) of the coarse fraction of NA was evaluated. Considering the results obtained, it is concluded:

I. The optimum SS/AC ratio was 1% (with respect to mass) to modify the AC.

II. At this percentage (SS/AC=1%), in the penetration and softening point tests, SS increased the stiffness of the base asphalt. However, the rheological properties and viscosity are similar.

III. The SS foams the binder at approximately 80°C, facilitating the covering of the aggregates. This contributes to a reduction in *VTM* at lower MT.

IV. The SS allows to decrease MT 20°C, generating a WMA mixture that exhibits similar or even better performance in certain properties compared to the Control HMA mixture.

V. SS contributes to increasing the resistance under monotonic loading (increases the *S/F* ratio, *ITSD*, and *ITSC* parameters) of asphalt mixtures (HMA and WMA). It also helped to increase resistance to moisture damage (increases *TSR*) and abrasion (decreases *CL*). However, from a statistical point of view, the results of these parameters in both mixtures are similar.

VI. Stiffness under cyclic loading, resistance to permanent deformation, and fatigue strength are similar for HMA and WMA mixtures.

VII. Replacing the 1/2” and 1/2”+3/8” NA particles with RCA resulted in a significant decrease in *ITSD*, *ITSC*, *TSR* (decreased indirect tensile strength and moisture damage resistance) and an increase in *CL* (decreased Cantabro abrasion resistance). Despite the above, the Marshall quotient (*S/F*) increased.

VIII. Mixtures with RCA experienced lower resilient modulus and fatigue strength, but similar resistance to deformation as the Control mixture (without RCA) from a statistical point of view.

IX. SS could contribute to produce a WMA that tends to be more environmentally friendly compared to HMA. This is because SS reduces the use of fuels and energy in asphalt plants, leading to lower emissions of greenhouse gases into the atmosphere and less environmental pollution.

X. Although RCA tends to decrease the strength and performance of HMA and WMA, its use as a replacement for 1/2” and 1/2”+3/8” NA particles can be seen as an environmentally sustainable alternative on roads with low traffic volumes.

Recommendations for future studies include: i) use different SiO_2/Na_2O concentrations, i.e., different types of SS; ii) evaluate long-term properties (aging, durability, etc.) of the WMA using SS; iii) conduct full-scale test and manufacture the WMA with the SS in an asphalt plant; iv) evaluate coat-ability of aggregate and foam quality; v) use different types of asphalt mixtures, AC, aggregates, recyclable materials to replace NA, gradations, etc., for the WMA; vi) use other types of RCA from different sources; vii) perform Life Cycle Cost Analysis (LCCA), Life Cycle Assessment (LCA), socio-economic and environmental impact assessment, etc., for the WMA; viii) evaluate the performance of the WMA mix at low temperatures.

Supplementary information ↑

Funding sources

Research carried out within the framework of Research Project 3-33-671-23 financed by the Universidad Distrital Francisco José de Caldas (Colombia).

Supplementary material

Not applicable.

Data availability

Not applicable.

Acknowledgements

The authors would like to thank the Oficina de Investigaciones of the Universidad Distrital Francisco José de Caldas for the support and resources obtained through Public Call 01-2023 (Research Project 3-33-671-23: “Development of a Warm mix asphalt – WMA with Recycled Concrete Aggregate – RCA”).

Authorship contribution statement

H.A. Rondón-Quintana: Conceptualization, Data curation, Formal analysis, Funding acquisition, Investigation, Methodology, Project administration, Resources, Supervision, Validation, Visualization, Writing - original draft, Writing - review & editing.

W.D. Fernández-Gómez: Formal analysis, Funding acquisition, Investigation, Writing - review & editing.

E.H. Sánchez-Cotte: Formal analysis, Funding acquisition, Investigation, Writing - review & editing.

Competing interests

The authors declare that they have no known financial conflicts of interest or personal relationships that could have influenced the work reported in this article.

Statement on the use of Artificial Intelligence

Not applicable.

REFERENCES

1. Rubio MC, Martínez G, Baena L, Moreno F. 2012. Warm mix asphalt: an overview. J. Clean. Prod. 24:76-84. https://doi.org/10.1016/j.jclepro.2011.11.053

2. Behnood A. 2020. A review of the warm mix asphalt (WMA) technologies: Effects on thermo-mechanical and rheological properties. J. Clean. Prod. 259:120817. https://doi.org/10.1016/j.jclepro.2020.120817

3. Ferrotti G, Mancinelli E, Passerini G, Canestrari F. 2024. Comparison of energy and environmental performance between warm and hot mix asphalt concrete production: A case study. Constr. Build. Mater. 418:135453. https://doi.org/10.1016/j.conbuildmat.2024.135453

4. Sukhija M, Saboo N. 2021. A comprehensive review of warm mix asphalt mixtures-laboratory to field. Constr. Build. Mater. 274:121781. https://doi.org/10.1016/j.conbuildmat.2020.121781

5. Sukhija M, Saboo N, Pani A. 2024. Suitability of warm mix asphalt (WMA) technologies based on performance and energy consumption. Road Mater. Pavement. Des. 25(7):1479–1506. https://doi.org/10.1080/14680629.2023.2268721

6. Sun G, Ning W, Jiang X, Qiu K, Cao Z, Ding Y. 2024. A comprehensive review on asphalt fume suppression and energy saving technologies in asphalt pavement industry. Sci. Total Environ. 913:169726. https://doi.org/10.1016/j.scitotenv.2023.169726

7. Araujo, DLV, Santos J, Martinez-Arguelles G. 2023. Environmental performance evaluation of warm mix asphalt with recycled concrete aggregate for road pavements. Int. J. Pavement Eng. 24(2):2064999. https://doi.org/10.1080/10298436.2022.2064999

8. Polo-Mendoza R, Martinez-Arguelles G, Peñabaena-Niebles R. 2023. Environmental optimization of warm mix asphalt (WMA) design with recycled concrete aggregates (RCA) inclusion through artificial intelligence (AI) techniques. Results Eng. 17:100984. https://doi.org/10.1016/j.rineng.2023.100984

9. Polo-Mendoza R, Peñabaena-Niebles R, Giustozzi F, Martinez-Arguelles G. 2022. Eco-friendly design of warm mix asphalt (WMA) with recycled concrete aggregate (RCA): A case study from a developing country. Constr. Build. Mater. 326:126890. https://doi.org/10.1016/j.conbuildmat.2022.126890

10. Polo-Mendoza R, Martinez-Arguelles G, Peñabaena-Niebles R, Covilla-Valera E. 2023. Neural networks implementation for the environmental optimisation of the recycled concrete aggregate inclusion in warm mix asphalt. Road Mater. Pavement. Des. 25(5):941–966. https://doi.org/10.1080/14680629.2023.2230298

11. Covilla-Varela E, Turbay E, Polo-Mendoza R, Martinez-Arguelles G, Cantero-Durango J. 2023. Recycled concrete aggregates (RCA)-based asphalt mixtures: A performance-related evaluation with sustainability-criteria verification. Constr. Build. Mater. 403:133203. https://doi.org/10.1016/j.conbuildmat.2023.133203

12. Liu Z, Feng T, Zhu X, Gao J, Hu K, Guo M, Gu F, Li F. 2024. Bird's-eye view of recycled solid wastes in road engineering. J. Road Eng. 4(2):93-150. https://doi.org/10.1016/j.jreng.2024.05.002

13. Kristjansdottir O, Muench S, Michael L, Burke GL. 2007. Assessing potential for warm-mix asphalt technology adoption. Transp. Res. Rec. 2040(1):91-99. https://doi.org/10.3141/2040-10

14. Sargand S, Nazzal MD, Al-Rawashdeh A, Powers D. 2012. Field evaluation of warm-mix asphalt technologies. J. Mater. Civ. Eng. 24(11):1343-1349. https://doi.org/10.1061/(ASCE)MT.1943-5533.0000434

15. Rondón-Quintana HA, Hernández-Noguera JA, Reyes-Lizcano FA. (2015). A review of warm mix asphalt technology: technical, economical and environmental aspects. Ing. Inv. 35(3):5-18. https://doi.org/10.15446/ing.investig.v35n3.50463

16. Cheraghian G, Falchetto AC, You Z, Chen S, Kim YS, Westerhoff J, Moon KH, Wistuba MP. 2020. Warm mix asphalt technology: An up to date review. J. Clean. Prod. 268:122128. https://doi.org/10.1016/j.jclepro.2020.122128

17. Hasan MRM, You Z, Yang X, 2017. A comprehensive review of theory, development, and implementation of warm mix asphalt using foaming techniques. Constr. Build. Mater. 152:115-133. https://doi.org/10.1016/j.conbuildmat.2017.06.135

18. Sukhija M, Saboo N, Pani A. 2023. Effect of warm mix asphalt (WMA) technologies on the moisture resistance of asphalt mixtures. Constr. Build. Mater. 369:130589. https://doi.org/10.1016/j.conbuildmat.2023.130589

19. Nithinchary J, Dhandapani BP, Mullapudi RS. 2024. Application of warm mix technology - design and performance characteristics: Review and way forward. Constr. Build. Mater. 414:134915. https://doi.org/10.1016/j.conbuildmat.2024.134915

20. Medeiros MS, Daniel JS, Bolton HL, Meagher WC. 2012. Evaluation of moisture and low-temperature cracking susceptibility of warm-mixture asphalt. Int. J. Pavement Eng. 13(5):395-400. https://doi.org/10.1080/10298436.2011.582113

21. Zhang K, Luo Y, Chen F., Han F. 2020. Performance evaluation of new warm mix asphalt and water stability of its mixture based on laboratory tests. Constr. Build. Mater. 241:118017. https://doi.org/10.1016/j.conbuildmat.2020.118017

22. Matinfar M, Nychka JA. 2023. A review of sodium silicate solutions: Structure, gelation, and syneresis. Adv. Colloid Interface Sci. 322:103036. https://doi.org/10.1016/j.cis.2023.103036

23. Liu S, Ott WK., 2020. Sodium silicate applications in oil, gas & geothermal well operations. J. Pet. Sci. Eng. 195:107693. https://doi.org/10.1016/j.petrol.2020.107693.

24. Wang JN, Fan ZT. 2010. Freezing–mechanical reclamation of used sodium silicate sands. Int. J. Cast Metals Res. 23(5):257-263. https://doi.org/10.1179/136404610X12665088537419

25. Lu G, Wang Y-S, Zhang Y, Ariaratnam ST. 2018. Feasibility of using sodium silicate as grouting in loose coal bed sections for methane drainage. Tunn. Undergr. Space Technol. 72:107-113. https://doi.org/10.1016/j.tust.2017.11.011

26. Avci E, Mollamahmutoğlu M, Deveci E. 2022. Sodium silicate-formamide grouted silt and silty sand properties. J. Adhes. Sci. Technol. 36(21):2269-2284. https://doi.org/10.1080/01694243.2021.2010879

27. Mollamahmutoğlu M, Avcı E, Deveci E, Gokce A, Yıldırım E. 2021. Strength and permeability properties of sodium silicate-sodium dihydrogen phosphate grouted sand. Arab. J. Geosci. 14:2061. https://doi.org/10.1007/s12517-021-08427-y

28. Wang H, Shu L, Ma K, He X. 2024. Durability improvement of pumice lightweight aggregate concrete by incorporating modified rubber powder with sodium silicate. Materials 17(4):786. https://doi.org/10.3390/ma17040786

29. Sun B, Zheng L, Li P, Sheng G, Li X, Zuo Y. 2022. Enhance of strengthening phase and chemical bonding in bamboo scrap/magnesium oxychloride composites by sodium silicate. Mater. Lett. 308(Part B):131275. https://doi.org/10.1016/j.matlet.2021.131275

30. Noritake F, Sato T, Yamamoto A, Wakabayashi D, Urakawa S, Funamori N. 2022. Structure of sodium silicate water glass—X-ray scattering experiments and force-field molecular dynamics simulations. J. Non-Cryst. Solids 579:121370. https://doi.org/10.1016/j.jnoncrysol.2021.121370

31. Gilford III J, Hassan MM, Rupnow T, Barbato M, Okeil A, Asadi S. 2014. Dicyclopentadiene and sodium silicate microencapsulation for self-healing of concrete. J. Mater. Civ. Eng. 26(5):886-896. https://doi.org/10.1061/(ASCE)MT.1943-5533.0000892

32. Cavusoglu I, Yilmaz E, Yilmaz AO. 2021. Sodium silicate effect on setting properties, strength behavior and microstructure of cemented coal fly ash backfill. Powder Technol. 384:17-28. https://doi.org/10.1016/j.powtec.2021.02.013

33. Min Y, Gao M, Yao C, Wu, J, Wei X. 2023. On the use of one-part geopolymer activated by solid sodium silicate in soft clay stabilization. Construction and Building Materials. 402:132957. https://doi.org/10.1016/j.conbuildmat.2023.132957

34. Ma C, Qin Z, Zhuang Y, Chen L, Chen B. 2015. Influence of sodium silicate and promoters on unconfined compressive strength of Portland cement-stabilized clay. Soils Found. 55(5):1222-1232. https://doi.org/10.1016/j.sandf.2015.09.021

35. Suganya K, Sivapullaiah PV. 2016. Role of sodium silicate additive in cement-treated Kuttanad soil. J. Mater. Civ. Eng. 28(6):06016006. https://doi.org/10.1061/(ASCE)MT.1943-5533.0001538

36. Vakili MV, Chegenizadeh A, Nikraz H, Keramatikerman M. 2016. Investigation on shear strength of stabilised clay using cement, sodium silicate and slag. Appl. Clay Sci. 124–125:243-251. https://doi.org/10.1016/j.clay.2016.02.019

37. Jiang P, Zheng W, Zhou L. Li N, Wang W. 2023. Laboratory characterization of soft clay mixed with EPS, lime, fly ash, and sodium silicate. Bull. Eng. Geol. Environ. 82:302. https://doi.org/10.1007/s10064-023-03297-y

38. Alizadeh S, Shafabakhsh G, Sadeghnejad M. 2023. Sustainable asphalt mixtures: Enhancing environmental impact by partial fine aggregate substitution with rubber powder and bitumen modification using Nano-SiO2. Int. J. Pavement Eng. 24(2):2257851. https://doi.org/10.1080/10298436.2023.2257851

39. Mohammed AM, Abed AH. 2023. Enhancing asphalt binder performance through nano-SiO_2 and nano-CaCO3 additives: Rheological and physical insights. Case Stud. Constr. Mater. 19:e02492. https://doi.org/10.1016/j.cscm.2023.e02492

40. Bhat FS, Gilani TA, Din IMU, Aziz G, Mir MS, Shah AH, Sheikh IR, Mudasir P. 2024. Integration of nano Al_2O_3 and nano SiO_2 in asphalt mixes: A comprehensive performance and durability evaluation. Constr. Build. Mater. 412:134687. https://doi.org/10.1016/j.conbuildmat.2023.134687

41. Farouk S, Abdel-Wahab F, Abdelmaksoud H, Abdel-Baki M, El-Faramawy N. 2024. Thermoluminescence properties study of double dopants borosilicate glasses: Transition metal (Cr_2O_3, ZnO) and alkaline metal (Na_2O). Opt. Mater. 149:115145. https://doi.org/10.1016/j.optmat.2024.115145

42. Yang C, Bai J, Wang G, Wang H, Ma S. 2023. Effect of Na_2O content on wettability, crystallization and performances of sealing glass. J. Mater. Res. Technol. 23:4117-4134. https://doi.org/10.1016/j.jmrt.2023.02.073

43. Arabani M, Azarhoosh AR. 2012. The effect of recycled concrete aggregate and steel slag on the dynamic properties of asphalt mixtures. Constr. Build. Mater. 35:1–7. https://doi.org/10.1016/j.conbuildmat.2012.02.036

44. Afshar T, Disfani MM, Arulrajah A, Narsilio GA, Emam S. 2017. Impact of particle shape on breakage of recycled construction and demolition aggregates. Powder Techn. 308:1–12. https://doi.org/10.1016/j.powtec.2016.11.043

45. Tam VWY. 2009. Comparing the implementation of concrete recycling in the Australian and Japanese construction industries. J. Clean. Prod. 17(7):688–702. https://doi.org/10.1016/j.jclepro.2008.11.015

46. Habibi A, Ramezanianpour AM, Mahdikhani M, Bamshad O. 2021. RSM-based evaluation of mechanical and durability properties of recycled aggregate concrete containing GGBFS and silica fume. Constr. Build. Mater. 270:121431. https://doi.org/10.1016/j.conbuildmat.2020.121431

47. Al-Bayati HKA, Tighe SL, Achebe J. 2018. Influence of recycled concrete aggregate on volumetric properties of hot mix asphalt. Resour. Conserv. Recycl. 130:200–214. https://doi.org/10.1016/j.resconrec.2017.11.027

48. Le HB, Bui QB. 2020. Recycled aggregate concretes – A state-of-the-art from the microstructure to the structural performance. Constr. Build. Mater. 257:119522. https://doi.org/10.1016/j.conbuildmat.2020.119522

49. Giri JP, Panda M, Sahoo UC. 2019. Development and evaluation of some bituminous mixes containing RCA. J. Test. Eval. 49(4):2579–2596. https://doi.org/10.1520/JTE20180824

50. Upshaw M, Cai CS. 2020. Critical review of recycled aggregate concrete properties, improvements, and numerical models. J. Mater. Civ. Eng. 32(11):03120005. https://doi.org/10.1061/(asce)mt.1943-5533.0003394

51. Tahmoorian F, Samali B. 2018. Laboratory investigations on the utilization of RCA in asphalt mixtures. Int. J. Pavement Res. Technol. 11(6):627-638. https://doi.org/10.1016/j.ijprt.2018.05.002

52. Xu X, Luo Y, Sreeram A, Wu Q, Chen G, Cheng S, Chen Z, Chen X. 2022. Potential use of recycled concrete aggregate (RCA) for sustainable asphalt pavements of the future: A state-of-the-art review. J. Clean. Prod.

344:130893. https://doi.org/10.1016/j.jclepro.2022.130893

53. Pasandín AR, Pérez I. 2015. Characterisation of recycled concrete aggregates when used in asphalt concrete: a technical literature review. Eur. J. Environ. Civ. Eng. 19(8):917–930. http://doi.org/10.1080/19648189.2014.985850

54. Bastidas-Martínez JG, Reyes-Lizcano FA, Rondón-Quintana HA. 2022. Use of recycled concrete aggregates in asphalt mixtures for pavements: A review. J. Traffic Transp. Eng. (Engl. Ed.) 9(5):725-741. https://doi.org/10.1016/j.jtte.2022.08.001

55. Li M, Xie J, Wu S, Chen J. 2023. Study on the influence mechanism of recycled concrete aggregate on strength of asphalt mixtures. Constr. Build. Mater. 400:132720. https://doi.org/10.1016/j.conbuildmat.2023.132720

56. Nwakaire CM, Yap SP, Yuen CW, Onn CC, Koting S, Babalghaith AM. 2020. Laboratory study on recycled concrete aggregate-based asphalt mixtures for sustainable flexible pavement surfacing. J. Clean. Prod. 262:121462. https://doi.org/10.1016/j.jclepro.2020.121462

57. Rondón-Quintana HA, Ruge-Cárdenas JC, Patiño DF, Vacca-Gamez, HA, Reyes-Lizcano FA, De Farias MM. 2018. Blast furnace slag as a substitute for the fine fraction of aggregates in an asphalt mixture. J. Mater. Civ. Eng. 30(10):04018244. https://doi.org/10.1061/(ASCE)MT.1943-5533.0002409

58. Rondón-Quintana HA, Ruge-Cárdenas JC, Reyes-Lizcano FA, Bastidas-Martínez JG, Zafra-Mejía CA. 2023. Mechanical resistance of hot-mix asphalt using phosphorite as filler. J. Mater. Civ. Eng. 35(9):04023274. https://doi.org/10.1061/JMCEE7.MTENG-15720

59. Hossain Z, Zaman M, O'Rear EA, Chen DH. 2012. Effectiveness of water-bearing and anti-stripping additives in warm mix asphalt technology. Int. J. Pavement Eng. 13(5):424-432. https://doi.org/10.1080/10298436.2011.616588

60. Wasiuddin NM, Selvamohan S, Zaman MM, Guegan MLTA. 2007. Comparative laboratory study of Sasobit and Aspha-min additives in warm-mix asphalt. Transp. Res. Rec. 1998(1):82-88. https://doi.org/10.3141/1998-10

61. Instituto Nacional de Vías – INVIAS. 2022. Especificaciones Generales de Construcción de Carreteras, Bogotá, D.C., Colombia.

62. Enieb M, Diab A. 2017. Characteristics of asphalt binder and mixture containing nanosilica. Int. J. Pavement Res. Technol. 10(2):148–157. https://doi.org/10.1016/j.ijprt.2016.11.009

63. Saltan M, Terzi S, Karahancer S. 2017. Examination of hot mix asphalt and binder performance modified with nano silica. Constr. Build. Mater. 156:976–984. https://doi.org/10.1016/j.conbuildmat.2017.09.069

64. Sun L, Xin X, Ren J. 2017. Inorganic nanoparticle-modified asphalt with enhanced performance at high temperature. J. Mater. Civ. Eng. 29(3):04016227. https://doi.org/10.1061/(ASCE)MT.1943-5533.0001750

65. Shafabakhsh GA, Sadeghnejad M, Ahoor B, Taheri E. 2020. Laboratory experiment on the effect of nano SiO_2 and TiO_2 on short and long-term aging behavior of bitumen. Constr. Build. Mater. 237:117640, https://doi.org/10.1016/j.conbuildmat.2019.117640

66. Cox BC, Smith BT, Howard IL, James RS. 2017. State of knowledge for Cantabro testing of dense graded asphalt. J. Mater. Civ. Eng. 29(10):04017174. https://doi.org/10.1061/(ASCE)MT.1943-5533.0002020

67. Karati S, Roy TK. 2022. Assessment of temperature impact on SDA modified bituminous concrete by non-destructive test. Mater. Today: Proc. 65(Part 8):3417-3423. https://doi.org/10.1016/j.matpr.2022.05.551

68. Liao G, Fang X, Wang H, Tang J, Szary P, Chen J. 2022. Durability improvement of poroelastic road surface with treated rubber: Molecular dynamics simulation and experimental observations. J. Clean. Prod. 369:133334. https://doi.org/10.1016/j.jclepro.2022.133334

69. Sanchez-Cotte EH, Fuentes L, Martinez-Arguellez G, Rondón-Quintana HA, Walubita LF, Cantero-Durango JM.2020. Influence of recycled concrete aggregates from different sources in hot mix asphalt design. Constr. Build. Mater. 259:120427. https://doi.org/10.1016/j.conbuildmat.2020.120427

70. Zuluaga-Astudillo DA, Rondón-Quintana HA, Zafra-Mejía CA. 2021. Mechanical performance of gilsonite modified asphalt mixture containing recycled concrete aggregate. Appl. Sci. 11(10):4409. https://doi.org/10.3390/app11104409

71. Sejin-Garces JE, Ahumada-Navarro G, Rondón-Quintana HA, Reyes-Lizcano FA, Bastidas-Martínez JG. 2024. Mechanical strength of and hot-mix asphalt using recycled concrete aggregate: mass and volume proportioning. Road Mater. Pavement. Des. 26(3),536–558. https://doi.org/10.1080/14680629.2024.2371338

72. Rondón-Quintana HA, Ruge-Cárdenas JC, Muniz de Farias M. 2019. Behavior of a hot mix asphalt containing blast furnace slag as aggregate: evaluation by mass and volume substitution. J. Mater. Civ. Eng. 31(2):04018364. https://doi.org/10.1061/(ASCE)MT.1943-5533.000257

73. Tang Q, Xiao P, Kou C, Lou K, Kang A, Wu Z. 2021. Physical, chemical and interfacial properties of modified recycled concrete aggregates for asphalt mixtures: A review. Constr. Build. Mater. 312:125357. https://doi.org/10.1016/j.conbuildmat.2021.125357

74. Mikhailenko P, Kakar RM, Piao Z, Bueno M, Poulikakos L. 2020. Incorporation of recycled concrete aggregate (RCA) fractions in semi-dense asphalt (SDA) pavements: volumetrics, durability and mechanical properties. Constr. Build. Mater. 264:120166. https://doi.org/10.1016/j.conbuildmat.2020.120166

75. Radević A, Đureković A, Zakić D, Mladenović G. 2017. Effects of recycled concrete aggregate on stiffness and rutting resistance of asphalt concrete. Constr. Build. Mater. 136:386-393. https://doi.org/10.1016/j.conbuildmat.2017.01.043

76. Radević A, Isailović I, Wistuba MP, Zakić D, Orešković M, Mladenović G. 2020. The impact of recycled concrete aggregate on the stiffness, fatigue, and low temperature performance of asphalt mixtures for road construction. Sustainability 12(10):3949. https://doi.org/10.3390/su12103949

77. El-Tahan D, Gabr A, El-Badawy S, Shetawy M. 2018. Evaluation of recycled concrete aggregate in asphalt mixes. Innov. Infrastruct. Solut. 3:20. https://doi.org/10.1007/s41062-018-0126-7

78. Barman M, Ghabchi R, Singh D, Zaman M, Commuri S. 2018. An alternative analysis of indirect tensile test results for evaluating fatigue characteristics of asphalt mixes. Constr. Build. Mater. 166:204–213. https://doi.org/10.1016/j.conbuildmat.2018.01.049

79. Bastidas-Martínez JG, Rondón-Quintana HA. 2024. Assessment of asphalt binder content, temperature and loading rate in indirect tensile strength and resilient modulus tests of a hot-mix asphalt – Comparison with Marshall design method. Constr. Build. Mater. 426:136158. https://doi.org/10.1016/j.conbuildmat.2024.136158

80. Bastidas-Martínez JG, Camapum de Carvalho J, Cristhiane LL, Muniz de Farias, M, Rondón-Quintana HA. 2022. Effects of iron ore tailing on performance of hot-mix asphalt. J. Mater. Civ. Eng. 34(1):04021405. https://doi.org/10.1061/(ASCE)MT.1943-5533.0004034

81. Bharath G, Reddy KS, Tandon V, Reddy MA. 2021. Aggregate gradation effect on the fatigue performance of recycled asphalt mixtures. Road Mater. Pavement. Des. 22(1):165-184. https://doi.org/10.1080/14680629.2019.1620116